Towards general-relativistic pulsar magnetospheres

Jérôme Pétri

Observatoire Astronomique de Strasbourg, Université de Strasbourg, France.

Physics of Neutron Stars, Saint-Petersbourg, 29/7/2014

Summary

1. Introduction
   - objectives
   - pulsar magnetospheres
2. The setup
   - background metric
   - Maxwell equations in 3+1 formalism
   - algorithm
3. Results
   - vacuum solutions
   - force-free solutions
4. Conclusion & Perspectives

Our goal

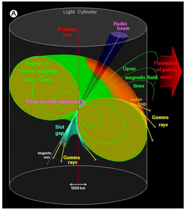

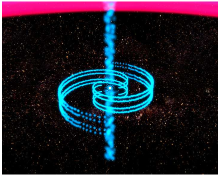

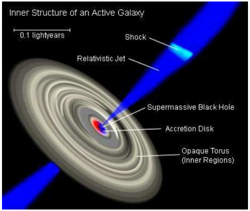

1. Objectives
   to construct pulsar magnetospheres
   - in general-relativity.
   - force-free limit.
   - extension to dissipative/resistive/MHD solutions.
2. Method
   full 3D numerical simulations
   - time-dependent evolution of the electromagnetic field.
   - 3+1 formalism in general relativity.
   - pseudo-spectral discontinuous Galerkin approximation.
3. Applications
   force-free field in curved space-time
   - pulsar.
   - black holes.

- Almost FFE simulation
  - force-free electromagnetic field.
  - time evolution of Maxwell equations.
  - current along **B** not included.
  - formation of a current sheet.
- Limitations
  - cartesian geometry even for the star surface.
  - ratio $R/r_{\rm L} = 0.2$ too large $\Rightarrow P = 1$ ms.
- Remedies

  $\Rightarrow$ use spherical geometry

  2D axisymmetric *(Parfrey et al., 2012)*

  full 3D *(Pétri, 2012)*

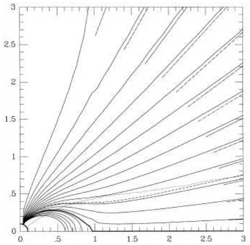

(Contopoulos et al., 1999)

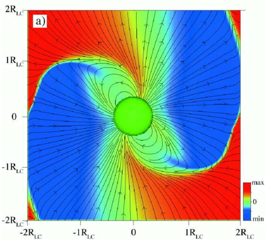

(Spitkovsky, 2006)

Resistive models

force-free magnetospheres do not allow dissipation or radiation
$\Rightarrow$ add some resistivity

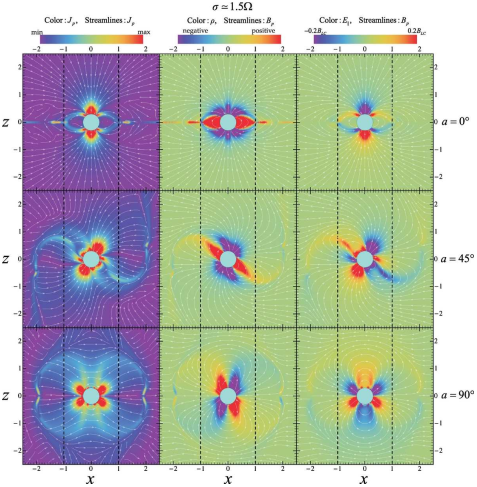

(Kalapotharakos et al., 2012)

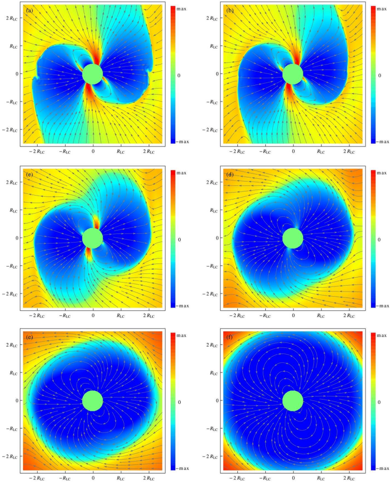

(Li et al., 2012)

Space-time curvature and frame dragging

modify the structure of the electromagnetic field close to the neutron star surface

- amplification of the intensity of the electric field in the neighborhood of the stellar surface because of the gravitational field
  (Muslimov & Tsygan, 1992).
- dynamics of the polar caps changed
  (Beskin, 1990).

Consequences on the magnetosphere

Quantitative modifications of

- the geometry of the polar caps, opening angle.
- the shape of the radio pulses.
- the modulation of the light-curves in X-rays for accreting pulsars.
- spin-down luminosity.
  (Pétri, 2013, 2014).

The background metric

Four dimensional space-time split into a 3+1 foliation such that

$$ds^2 = g_{ik} \, dx^i \, dx^k = \alpha^2 \, c^2 \, dt^2 - \gamma_{ab} \, (dx^a + \beta^a \, c \, dt) \, (dx^b + \beta^b \, c \, dt)$$

with coordinate basis $x^i = (c\,t, x^a)$, t is the time coordinate or universal time and x^a some associated space coordinates.

- lapse function α.
  For a slowly rotating neutron star

$$\alpha = \sqrt{1 - \frac{R_s}{r}}$$

- shift vector β

$$c\,\beta = -\,\omega\, r\, \sin\vartheta\, \vec{e}_\varphi$$

$$\omega = \frac{R_s\, a\, c}{r^3}$$

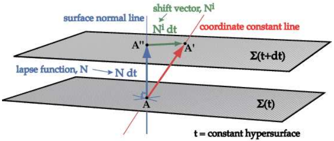

(Shinkai, 2009)

Maxwell equations in 3+1 formalism

Maxwell equations in curved space-time are similar to those in matter

$$\begin{aligned}
\operatorname{div} \mathbf{B} &= 0 \\
\mathbf{rot}\, \mathbf{E} &= -\frac{1}{\sqrt{\gamma}}\, \partial_t(\sqrt{\gamma}\, \mathbf{B}) \\
\operatorname{div} \mathbf{D} &= \rho \\
\mathbf{rot}\, \mathbf{H} &= \mathbf{J} + \frac{1}{\sqrt{\gamma}}\, \partial_t(\sqrt{\gamma}\, \mathbf{D})
\end{aligned}$$

(Komissarov, 2004)

Differential operators defined in a three dimensional curved space, the absolute space with associated spatial metric γ_{ab}

$$\begin{aligned}
\operatorname{div} \mathbf{B} &\equiv \frac{1}{\sqrt{\gamma}}\, \partial_a(\sqrt{\gamma}\, B^a) \\
\mathbf{rot}\, \mathbf{E} &\equiv e^{abc}\, \partial_b\, E_c \\
\mathbf{E} \times \mathbf{B} &\equiv e^{abc}\, E_b\, B_c
\end{aligned}$$

Constitutive relations

- three dimensional vector fields are not independent, they are related by two important constitutive relations

$$\varepsilon_0 \, \mathbf{E} = \alpha \, \mathbf{D} + \varepsilon_0 \, c \, \beta \times \mathbf{B}$$

$$\mu_0 \, \mathbf{H} = \alpha \, \mathbf{B} - \frac{\beta \times \mathbf{D}}{\varepsilon_0 \, c}$$

- curvature of absolute space taken into account by
  - lapse function factor α in the first term.
  - frame dragging effect in the second term, cross-product between the shift vector β and the fields.

- $(\mathbf{D}, \mathbf{B})$ are the fundamental fields measured by a FIDO. The force-free current density is

$$\mathbf{J} = \rho \, \frac{\mathbf{E} \times \mathbf{B}}{B^2} + \frac{\mathbf{B} \cdot \mathrm{rot}\, \mathbf{H} - \mathbf{D} \cdot \mathrm{rot}\, \mathbf{E}}{B^2} \, \mathbf{B}$$

$$\alpha \, \mathbf{j} = \mathbf{J} + \rho \, c \, \beta$$

Numerical method

Pseudo-spectral discontinuous Galerkin method

- finite volume formulation in radius.
- high-order interpolation with Legendre polynomials.
- non uniform radial grid (high resolution where needed).
- spectral interpolation in longitude/latitude.
- vector spherical harmonic decomposition.
- 4th order Runge-Kutta time integration.
- Lax-Friedrich flux.
- stabilization by filtering and limiting (avoid overshoot/oscillations).
- exact boundary conditions on the neutron star surface.
- outgoing waves at the outer boundary.

Tested against

- vacuum monopole and Deutsch solution.
- force-free monopole/split monopole.

(Pétri, 2012)

Vacuum solutions

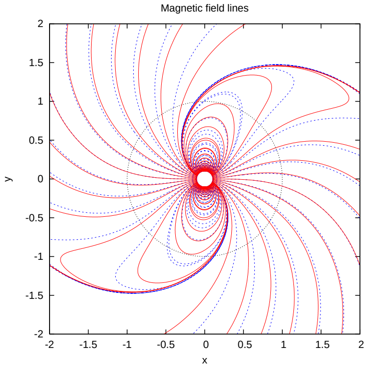

Figure : Vacuum magnetic field lines of the perpendicular rotator in the equatorial plane for $r_L/R = 10$ (flat space-time in blue).

(Pétri, 2014)

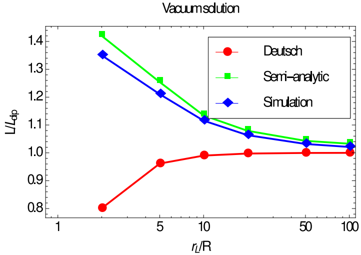

Figure : Normalized Poynting flux $L/L_{\rm dip}$ for the perpendicular rotator compared to the Deutsch solution. (Corrections for Ω-redshift and B-amplification omitted, see *(Rezzolla & Ahmedov, 2004)*).

Spin parameter

$$\frac{a}{R_s} = \frac{2}{5}\,\frac{R}{R_s}\,\frac{R}{r_L}$$

with $R = 2\,R_s$.

The (split) monopole solutions: magnetic field and Poynting flux

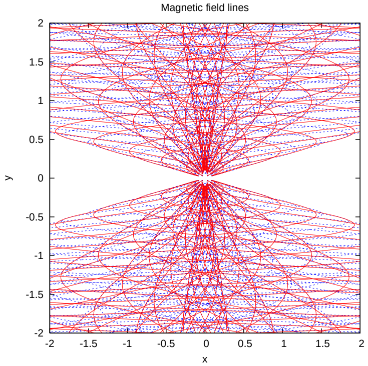

Figure : Force-free magnetic field lines of the split monopole in the meridional plane for $r_L/R = 10$ (flat space-time in blue).

(Pétri, submitted)

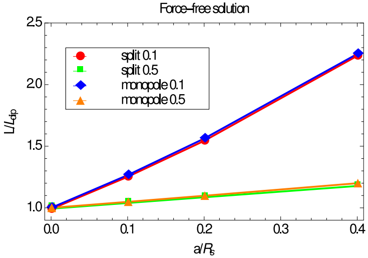

Figure : Normalized Poynting flux $L/L_{\rm mono}$ for monopole/split monopole and dipole in general relativity. (Ω-redshift and B-amplification included)

(Pétri, in preparation)

Dipolar geometry: magnetic field and Poynting flux

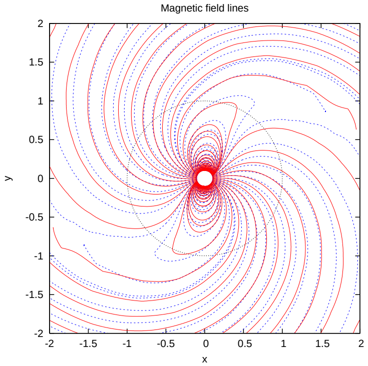

Figure : Force-free magnetic field lines of the perpendicular rotator in the equatorial plane for $r_{\rm L}/R = 10$ (flat space-time in blue).

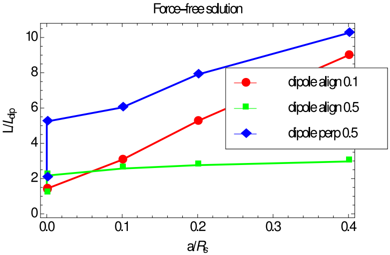

Figure : Normalized Poynting flux $L/L_{\rm mono}$ for monopole/split monopole and dipole in general relativity. (Ω-redshift and B-amplification included)

(Pétri, in preparation)

Preliminary low resolution results

Conclusions & Perspectives

Vacuum and force-free fields

- fully 3D general-relativistic force-free pulsar magnetosphere.
- spin-down luminosity increased by a significant amount compared to flat space-time.
- be careful about the point dipole magneto-losses formula.
- phase lag in the magnetic field structure
  $\Rightarrow$ implications for radio and high-energy pulse phase lag?

Magnetospheres of compact objects

- more realistic assumptions for the plasma
  $\Rightarrow$ relaxation of the force-free condition.
- GRMHD simulations.
- resistive magnetospheres.

Beskin V. S., 1990, Soviet Astronomy Letters, 16, 286

Contopoulos I., Kazanas D., Fendt C., 1999, ApJ, 511, 351

Kalapotharakos C., Kazanas D., Harding A., Contopoulos I., 2012, ApJ, 749, 2

Komissarov S. S., 2004, MNRAS, 350, 427

Li J., Spitkovsky A., Tchekhovskoy A., 2012, ApJ, 746, 60

Muslimov A. G., Tsygan A. I., 1992, MNRAS, 255, 61

Parfrey K., Beloborodov A. M., Hui L., 2012, MNRAS, 423, 1416

Pétri J., 2012, MNRAS, 424, 605

Pétri J., 2013, MNRAS, 433, 986

Pétri J., 2014, MNRAS, 439, 1071

Rezzolla L., Ahmedov B. J., 2004, MNRAS, 352, 1161

Shinkai H., 2009, Journal of Korean Physical Society, 54, 2513

Spitkovsky A., 2006, ApJL, 648, L51